Influence of Mach Number on Tornado Corner Flow Dynamics

J. XIA,* W. S. LEWELLEN, AND D. C. LEWELLEN

Department of Mechanical and Aerospace Engineering, West Virginia University, Morgantown, West Virginia

(Manuscript received 14 August 2002, in final form 5 June 2003)

ABSTRACT

Since maximum Mach numbers in an F5 tornado are expected to, at least, reach ~0.4, a study was undertaken to determine the major potential compressibility effects in such flows. Results from compressible large-eddy simulations of tornado corner flow dynamics are summarized. Comparison with previous incompressible simulations indicates that Mach number effects tend to be modest and may be estimated by an isentropic approximation. As the average maximum Mach number *M* within the tornado increases above one-half, the largest changes occur for ''low-swirl'' corner flows, those exhibiting a central vertical jet off the surface capped by a vortex breakdown, with the vortex breakdown found to occur at significantly greater heights as *M* increases. It also appears that the highest Mach numbers are most likely to occur during rapid transients in near-surface intensification that can sometimes occur during a tornado's evolution.

1. Introduction

There has long been speculation about what maximum wind speeds are achievable in extreme tornadoes. A recent review (Davies-Jones et al. 2001) cites a limit on observations for F5 tornadoes of between 125 and 140 m s^{-1}, with these values somewhat larger than the so-called *thermodynamic speed limit* based on convective available potential energy (CAPE) in the storm environment. This would appear to limit the maximum Mach number to <~0.5. Already this is high enough to suggest that compressibility effects may modestly alter the tornado flow structure, and there are reasons to question whether even higher Mach numbers could be reached. First, the observations involve considerable spatial and temporal averaging. Second, Lewellen et al. (2000a) have shown that the interaction of a tornado with the surface can lead to significant near-surface intensification: low-level swirl velocities up to 2.5 times the maximum swirl velocity aloft and vertical velocities an additional factor of 1.4 larger yet. These velocities occur in the corner flow region, where the vortex core meets the surface and the surface layer inflow turns up into the central core of the tornado. Much higher near-surface intensifications appear possible in a particular unsteady process that we refer to as ''corner flow collapse'' (Lewellen et al. 2000b; Lewellen and Lewellen 2002). The name refers to rapid reduction in vortex core radius near the surface that can be produced in response to a restriction in the boundary layer inflow. Thus, it seems possible that local Mach numbers may markedly exceed that estimated by simply dividing the speed based on storm available potential energy by the environmental speed of sound. Fiedler (1996) used an axisymmetric, laminar vortex model to argue that speeds in a tornado need not be limited to the speed of sound. He suggested that transonic flow conditions might be found within the secondary vortices seen in some tornadoes.

In view of the potential for extreme wind speeds in some tornadoes, a fully compressible study (Xia 2001), directly comparable to our incompressible tornado corner flow large-eddy simulations (LES; Lewellen et al. 2000a), was performed to see what Mach numbers might induce significant dynamical changes in the tornado corner flow, and to determine the character of those changes. This study serves to check the range of validity of the previous incompressible results. It also tests whether compressible effects might significantly limit the magnitude of wind speeds that can be reached or provide unique signatures of high speeds that might be searched for in the field.

The development and testing of the compressible tornado code are briefly described in the next section, followed by a section that summarizes the most important results from a number of simulations. A detailed report of these topics is given by Xia (2001).

* Current affiliation: Fluent Incorporated, Lebanon, New Hampshire.

Corresponding author address: W. Steve Lewellen, Dept. of Mechanical and Aerospace Engineering, West Virginia University, P.O. Box 6106, Morgantown, WV 26506-6106.
E-mail: WSLewellen@mail.wvu.edu

2. Model development and validation

a. Basic model

The compressible LES model was developed to study the potential influence of compressibility on the tornado model simulations given by Lewellen et al. (1997) and Lewellen et al. (2000a). These LES simulations incorporated a fine grid resolution (down to ~1 m) in a relatively small domain (~1 km^3) to study the interaction of a tornado with the surface. The only difference between the model used for these previous incompressible simulations and the current compressible model is the replacement of the constant density assumption with a constant potential temperature assumption. Although the model formulated in Xia (2001) includes the possibility of variable potential temperature, all of the tornado simulation results considered here assume a constant value for the potential temperature, $\theta \equiv T(P_0/P)^{R/C_p} = T/\pi$, for temperature T, pressure P, constant reference pressure P_0, specific heat at constant pressure C_p, and gas constant R. In this approximation, the two conservation equations to be solved by the model may be written as mass conservation:

$$\frac{C_v}{R\pi}\left(\frac{\partial \pi}{\partial t} + u_i\frac{\partial \pi}{\partial x_i}\right) + \frac{\partial u_i}{\partial x_i} = 0, \tag{1}$$

and momentum conservation:

$$\frac{\partial u_i}{\partial t} + u_j\frac{\partial u_i}{\partial x_j} = -C_p\theta\frac{\partial \pi}{\partial x_i} + \frac{\partial \tau_{ij}}{\partial x_j}, \tag{2}$$

where C_v is specific heat at constant volume, and τ_{ij} is the modeled subgrid flux terms for momentum. Note that we have ignored the gravitational term in Eq. (2) to be consistent with the analysis of Lewellen et al. (2000a) where it is assumed that within the corner flow, buoyant forcing is negligible in comparison to pressure gradient forcing.

Because $C_pR\theta\pi/C_v = a^2$, the speed of sound squared, it may be argued from Eq. (2) that perturbations in π will be of order Mach number squared. Thus, for flows with sufficiently small Mach numbers everywhere, the term in parenthesis on the left-hand side of Eq. (1) may be approximated as zero, and Eq. (1) reduces to the incompressible continuity equation. The π gradient in Eq. (2) is equal to the familiar pressure gradient term used in our earlier incompressible studies as long as θ is constant for any value of Mach number; that is,

$$C_p\theta\frac{\partial \pi}{\partial x_i} = \frac{1}{\rho}\frac{\partial P}{\partial x_i}. \tag{3}$$

It follows that any of the results of our previous incompressible study may be transformed to an isentropic approximation for sufficiently low Mach numbers. Such transformed results will be compared with the current compressible simulations in the next section to provide an idea of how good this approximation of neglecting the π gradients in Eq. (1) is for different Mach numbers.

We found it easier to keep the mass and momentum accurately conserved in the finite difference approximations to Eqs. (1) and (2) when using the density ρ and the velocity times the density $U_i = \rho u_i$ as the primary variables. So Eqs. (1) and (2) were written as

$$\frac{\partial \rho}{\partial t} + \frac{\partial U_i}{\partial x_i} - \frac{\partial}{\partial x_j}\left(K\frac{\partial \rho}{\partial x_j}\right) = 0, \tag{4}$$

$$\frac{\partial U_i}{\partial t} + \frac{\partial (U_iu_j)}{\partial x_j} = -\gamma R\theta\left(\frac{\rho}{\rho_0}\right)^{\gamma-1}\frac{\partial \rho}{\partial x_i} + \frac{\partial}{\partial x_j}\left[\nu\rho\left(\frac{\partial u_i}{\partial x_j} + \frac{\partial u_j}{\partial x_i}\right) - \frac{\rho q^3}{3}\delta_{ij}\right], \tag{5}$$

where K and ν are the subgrid diffusivities, $\rho q^2/2$ is the subgrid turbulent kinetic energy, δ_{ij} is the Kronecker delta, and $\gamma = C_p/C_v$. The subgrid model, which utilizes an equation for q^2, remains identical to that used by Lewellen et al. (2000a); subgrid velocity differences are assumed to be smaller than the resolved velocity differences so an incompressible treatment of the subgrid turbulence is still appropriate. The ρ diffusion term in Eq. (4) comes from modeling the correlation of the subgrid-scale fluctuations of the velocity and density.

The numerical model is a standard, second-order accurate, finite difference model, using the advection scheme of Piacsek and Williams (1970) on a staggered grid stretched in three dimensions and leapfrog time-differencing. A small amount (2%) of mixing between adjacent time steps is applied to remove the time-splitting instability of the leapfrog method. In order to insure that the finite difference scheme conserves mass and momentum exactly in each grid cell, the divergence form was adopted to discretize the advection term following Morinishi et al. (1998). A variable time step is employed, and, to maintain stability, it is chosen to satisfy a modified Courant condition for all grid cells:

$$\Delta t < \min\left(\frac{\Delta x_i}{|u_i| + a}\right). \tag{6}$$

As in Lewellen et al. (1997), relatively simple boundary conditions are chosen that are representative of the conditions that can occur on approximately a 1-km^3 domain within tornadic flows. In most of the simulations, quasi-steady-state conditions are sought, so the initial conditions are not too critical. For computational efficiency, the flow is allowed to spin up on a relatively coarse grid first before refining the inner mesh containing the corner flow region.

No variation in θ is included in any particular simulation, although the constant value of θ is changed to vary the speed of sound for different Mach number cases. Uniform θ is employed in the boundary conditions and any entropy generated by turbulence or shock dissipation is neglected, which should be a reasonable assumption as long as the maximum velocities are limited to low supersonic values or below.

b. Model verification

The accuracy and numerical stability of the compressible LES model have been verified in different ways. First several one-dimensional shock and expansion wave cases were used to check the compressible characteristics. Simulation results successfully matched the known analytical solutions. Second, the compressible code was also applied to simulate a two-dimensional purely swirling vortex, where its two-dimensional stability in low and high Mach number cases was checked. Then results from the compressible and incompressible codes were compared in a three-dimensional tornado vortex at very low Mach number, where they should closely match each other. Although the boundary conditions for these test cases were one-, two-, and three-dimensional, respectively, the code was always tested in three dimensions. Good agreement was achieved in all of the test cases, as detailed in Xia (2001).

3. Results

a. Quasi-steady cases

A major result of Lewellen et al. (2000a) was the demonstration that the character of the tornado wind field near the surface is largely governed by the corner flow swirl ratio S_c, defined in their Eq. (6) as a ratio of a characteristic swirl velocity to flow-through velocity for the surface-layer/corner/core component of the flow field. Peak quasi-steady, near-surface intensification was found to occur at $S_c \sim 1.3$ where a strong central jet between the surface and a capping vortex breakdown includes a maximum vertical velocity that is ~3.5 times the maximum swirl velocity aloft. Since the tornado corner flow velocity field depends so strongly on the corner flow swirl ratio the influence of Mach number may also be expected to depend strongly on S_c. In Xia (2001), detailed results for Mach number variation in corner flows with low ($S_c \sim 1.4$), medium ($S_c \sim 3$), and high ($S_c \sim 7$) swirl were exhibited. We will show only the most interesting results here.

A comparison of Mach number effects are shown in Fig. 1 for tornado corner flows with high swirl ratios ($S_c \sim 7$). The average pressure difference from the pressure at an outer reference radius normalized by $\rho_s V_s^2$ (density times the swirl velocity squared at that radius), is shown as a function of radius at a fixed height (15 m above the surface) where the lowest average pressure occurs for the incompressible case. Both axisymmetric and time averaging of the fully three-dimensional, unsteady simulations are used, with a sufficiently long simulation for the average result to have become steady. Each simulation is labeled by *M*, its maximum average Mach number. Both the incompressible distribution and its isentropic transforms are shown for comparison. For the isentropic transform model, the velocity distribution stays the same as the incompressible and, following Eq. (3), the pressure distribution may be approximated as

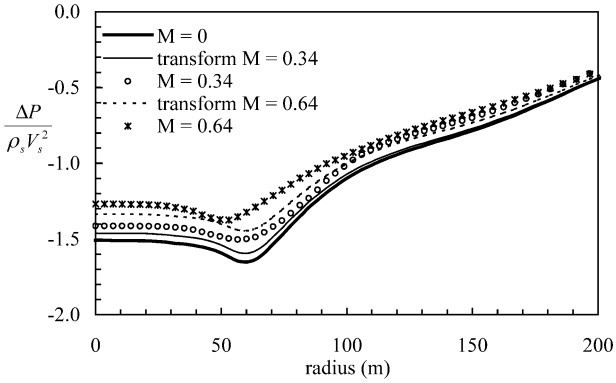

FIG. 1. Axisymmetric, time-averaged distribution of $\Delta P/(\rho_s V_s^2)$ vs radius at the fixed height where the lowest pressure occurs for a high swirl ratio tornado vortex.

$$\frac{\Delta P}{\rho_s V_s^2} = \frac{P_0}{\rho_s V_s^2}(\pi^{C_p/R} - 1) = \frac{P_0}{\rho_s V_s^2}\left[\left(1 + \frac{\Delta P_{\text{in}}/\rho_{\text{in}}}{C_p \theta}\right)^{C_p/R} - 1\right], \quad (7)$$

where the pressure drop between the stagnation pressure and the reference point has been neglected in comparison to the pressure drop at smaller radii.

Figure 1 shows that increasing *M* tends to yield a lower normalized pressure drop for small radii, due to the somewhat lower density reducing the outward inertia leading to most of the pressure drop. It should be noted that although the normalized centerline pressure drop is reduced as the Mach number is increased, the absolute pressure drop increases, because V_s needs to be increased to achieve the higher Mach number for constant sound speed. This figure also shows that only including the density drop in the momentum equation (i.e., the isentropic transform of the incompressible solution) tends to underestimate the Mach number effect. Even at the highest Mach number shown, the compressibility effects are not large, in spite of the fact that instantaneous local values of Mach number sometimes exceed one in some of the secondary vortices, consistent with the suggestion by Fiedler (1996) that transonic flow might occur in the secondary vortices of strong tornadoes. The instantaneous flow structure (not shown) was found to be qualitatively the same as in the incompressible case with several secondary vortices rotating about the center of the main vortex [cf. Fig. 5-4-4 of Xia (2001) and Fig. 2 of Lewellen et al. (2000a)].

In low swirl ($S_c \sim 1.4$) tornado corner flows, the minimum pressure usually occurs near the centerline, so the distribution of ΔP (normalized as in Fig. 1) is shown in Fig. 2 as a function of height along the vortex centerline. Both the isentropic transformations from the incompressible result and the results from the compressible runs show qualitatively similar decrease in pressure drop with increasing Mach number, but some-

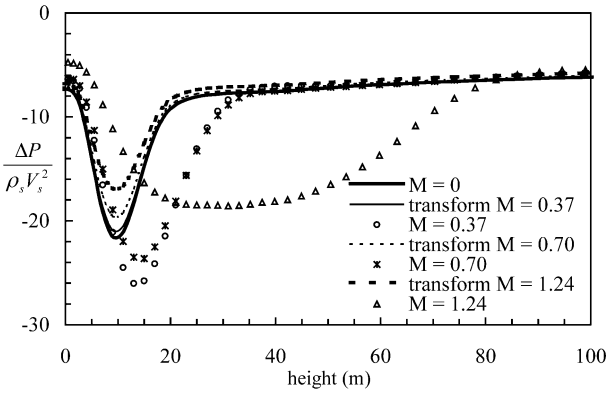

FIG. 2. Axisymmetric, time-averaged distribution of $\Delta P/(\rho_s V_s^2)$ vs height along the centerline in a low swirl ratio tornado vortex.

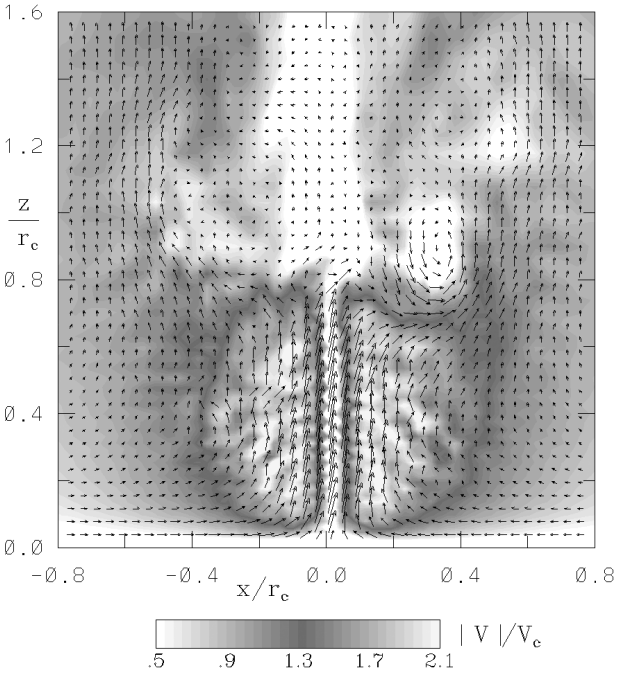

FIG. 3. Instantaneous vertical cross section of compressible low-swirl tornado vortex at large Mach number showing normalized swirl velocity (grayscale) and magnitude of the velocity vector in the *r–z* plane (arrows interpolated onto a uniform grid for clarity; maximum length corresponds to $V_{rz}/V_c = 3.60$).

what surprisingly the low Mach number compressible result shows a significantly greater pressure drop than the incompressible case. This is probably a result of the sharp peaking of the low-level pressure drop near the critical value of corner flow swirl ratio ($S_c^* \sim 1.3$) seen in Fig. 8 of Lewellen et al. (2000a). In this current series of low swirl ratio simulations, the local swirl ratio S_c is sufficiently close to S_c^* that a very small change in boundary conditions would be enough to modify the incompressible minimum pressure drop in Fig. 2 to values close to that for the low Mach number case. It is also possible for the density decrease associated with increasing Mach number to cause a slight effective shift in S_c, leading to an increased pressure drop in this region of great sensitivity to S_c. Unfortunately, the boundary conditions may not have been matched precisely enough in this low-swirl series of tests to limit the changes to compressibility effects.

One can see that the height where $\Delta P_{\min}$ locates in Fig. 2 and the vertical depth of the sharply reduced pressure region increase as the Mach number is increased. This correlates with an increase in the vortex breakdown height, which is associated with an increase in $W_{\max}/V_{\max}$ that occurs within the flow as Mach number increases. Above the breakdown the compressibility effects are small and the values of ΔP are close to each other at different Mach numbers.

An instantaneous view of the low-swirl, high Mach number case is shown in Fig. 3. Here the lengths are normalized by the upper core size r_c and the velocities by the maximum swirl velocity V_c in the flow above the corner flow, for ease of comparison with the corresponding incompressible view in Fig. 5 of Lewellen et al. (2000a). The most striking difference is the increase in the height of the breakdown by about a factor of 4. The much higher and stronger surface jet relative to the incompressible case is apparently forced by the need to conserve mass flux in the corner flow region while the density drops dramatically at high Mach number. The required increased volume flux is achieved by increasing both the vertical velocity and the core size. Although instantaneous local Mach numbers in excess of 1 are reached, there is no clear signature of shock waves occurring; it is not possible to distinguish shock gradients from the gradients occurring within the vortex breakdown itself.

The lowest pressures and highest Mach numbers occur near the centerline about half way between the surface and the vortex breakdown. The height of the breakdown is unsteady with the average height $\sim 0.6\, r_c$, while the instantaneous value at the time of Fig. 3 is somewhat higher. The ratio of maximum velocity to peak swirl velocity aloft for this case is raised to ~ 3.7. Since this maximum velocity occurs where the speed of sound has been reduced to its lowest value, the quasi-steady surface amplification of the time-averaged maximum Mach is even larger, ~ 4.4.

The medium-swirl case (shown in Xia 2001, for $S_c \sim 3$, and M up to 1) shows results that are between those for the high- and low-swirl cases. The minimum pressures occur at the centerline off the surface with a small increase in this height with increasing M. The relative change in the normalized pressure drop is similar to that shown for the low-swirl case, but the near-surface intensification factor remains much smaller. The most important observation in all cases is that, even with M approaching 1 the modifications in average velocity and pressure are not particularly significant.

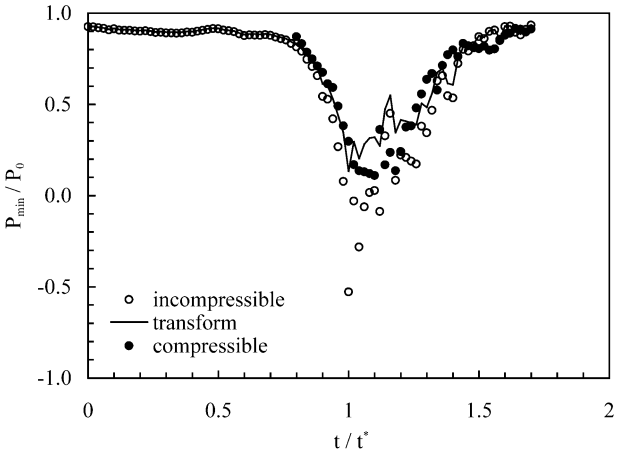

FIG. 4. Normalized minimum pressure (P_{min}/P_0) as a function of time (t/t^*) for the incompressible and compressible results during corner flow collapse ($t^* = r_d^2/\Gamma_0 \sim 100$ s for $r_d \sim 1$ km and $\Gamma_0 \sim 10^4$ m^2 s^{-1}).

b. A transient tornado evolution

Compressibility effects are potentially most important when a collapse of the tornado corner flow yields near-surface intensifications much higher than are possible under quasi-steady conditions. An example of this is case 1 in Lewellen et al. (2000b). The initial state was a very low-swirl ($S_c \sim 0.8$) corner flow, generated by enhancing the low-swirl, near-surface radial inflow in an otherwise high-swirl flow. Initially there is only a weak vortex at low levels, but impeding the low-level, low-swirl flow (as might happen, e.g., if a cold downdraft reached the surface and partially wrapped around the central flow) triggers an evolution of the corner flow from very low to high swirl generating a rapid collapse of the corner flow with corresponding intensification of the low-level velocities.

We resimulated this case with fully compressible flow, reducing the ambient speed of sound to 174 m s^{-1}, to highlight the compressible effects. Figure 4, normalized so that it should hold for different values of the speed of sound, shows that the peak pressure drop is significantly reduced, although the peak velocity actually increased. For the evolution shown in Fig. 4, we have found the minimum pressure in the incompressible case to be more sensitive to grid resolution than the corresponding compressible result. As long as the flow is strictly incompressible the principal limit on how small the local vortex core can become appears to be supplied by the grid resolution (at least down to the 2-m resolution considered here), but the decreasing density in the compressible case imposes a limit on minimum vortex core sizes as the Mach number increases. This limit on the minimum radius in turn constitutes a limit on the minimum pressure. The isentropically transformed incompressible points appear to give a relatively close estimate for the compressible values in this case. Although minimum pressures as low as 20% of P_0 are much lower than believed to be associated with tornadoes, it is important to note that the minimum pressures near the top of our domain (supplied by the storm aloft) do not drop below ~94% of P_0. It is the strong near-surface intensification associated with the collapsing corner flow that allows the local transient peak in minimum pressure to occur for a short period. The combination of the strong vertical pressure gradients associated with the vortex breakdown and strong radial pressure gradients associated with the swirl brought in by the collapsing corner flow permit the lower than expected values to be reached.

An instantaneous maximum local Mach number of almost 2.0 was reached at the time of minimum pressure in Fig. 4 (Xia 2001), corresponding to a surface intensification factor in maximum Mach number of over 9. The dynamics of transonic swirling flow are quite different from that of simple one-dimensional transonic flow, with Mach numbers permitted to exceed 1 within the minimum flow cross section, as shown by Lewellen et al. (1969). Their analysis shows that the maximum Mach number occurring in transonic swirling flow depends on the detailed distribution of angular momentum and total pressure across the streamlines flowing through the minimum cross section and that a value of 2 is well within an expected reasonable range.

4. Concluding remarks

Based on our simulation comparisons, we conclude that compressibility effects are unlikely to change the basic dynamics of tornadic corner flows even if Mach numbers greater than one are achieved. The most dramatic effects occur for low swirl ratios with a significant increase in the maximum vertical velocity and in the height of the vortex breakdown above the surface. The effects for medium- and high-swirl corner flows are not as large with the effect on high-swirl corner flow essentially limited to influencing the secondary vortices.

The compressibility effects may be estimated by an appropriate isentropic transformation applied to the incompressible results. This approximation leaves the velocity field unchanged and the reduced density yields an estimate of the reduction in pressure drop within the tornado. It misses the changes in the velocity field forced by the decreasing density as the Mach number is increased. The compressible simulations suggest that these velocity modifications can override the expected isentropic effects on pressure drop at some points in space for certain combinations of S_c and M.

This study leaves open the question of whether transonic velocities can actually occur in any tornadoes (Lewellen et al. 2002). We found no readily apparent physical barrier to such velocities occurring on rare occasions, since our simulations show that the basic flow structure is not drastically changed when velocities reach or exceed the local speed of sound, and the large near-surface intensification factors shown to occur mean

that it is not necessary for the driving supercell storm to have extremely large available energy. Given the location and duration of the highest velocities in tornado corner flows, any transonic velocities that might occur would be extremely difficult to observe in an actual tornado. Of course, it is also possible that physics not included in the model, such as the influence of dense debris, might reduce the chance of any transonic velocities.

Acknowledgments. This research was supported by National Science Foundation Grant 9317599 with S. P. Nelson as technical monitor.

REFERENCES

Davies-Jones, R., R. J. Trapp, and H. B. Bluestein, 2001: Tornadoes and tornadic storms. *Severe Convective Storms,* C. A. Doswell, Ed., Amer. Meteor. Soc., 167–221.

Fiedler, B., 1996: The sonic speed limit of tornadoes. Preprints, *18th Conf. on Severe Local Storms,* San Francisco, CA, Amer. Meteor. Soc., 385–386.

Lewellen, D. C., and W. S. Lewellen, 2002: Near-surface intensification during unsteady tornado evolution. Preprints, *21st Conf. on Severe Local Storms,* San Antonio, TX, Amer. Meteor. Soc., 481–484.

——, ——, and J. Xia, 2000a: The influence of a local swirl ratio on tornado intensification near the surface. *J. Atmos. Sci.,* **57,** 527–544.

——, ——, and ——, 2000b: Nonaxisymmetric, unsteady tornadic corner flows. Preprints, *20th Conf. on Severe Local Storms,* Orlando, FL, Amer. Meteor. Soc., 265–268.

Lewellen, W. S., W. J. Burns, and H. J. Strickland, 1969: Transonic swirling flow. *AIAA J.,* **7,** 1290–1297.

——, D. C. Lewellen, and R. I. Sykes, 1997: Large-eddy simulation of a tornado's interaction with the surface. *J. Atmos. Sci.,* **54,** 581–605.

——, J. Xia, and D. C. Lewellen, 2002: Transonic velocities in tornadoes? Preprints, *21st Conf. on Severe Local Storms,* San Antonio, TX, Amer. Meteor. Soc., 535–538.

Morinishi, Y., T. S. Lund, O. V. Vasilyev, and P. Moin, 1998: Fully conservative higher order finite difference schemes for incompressible flow. *J. Comput. Phys.,* **143,** 90–124.

Piacsek, S. A., and G. P. Williams, 1970: Conservative properties of convection difference schemes. *J. Comput. Phys.,* **6,** 392–405.

Xia, J., 2001: Large-eddy simulation of a three-dimensional, compressible tornado vortex. Ph.D. thesis, West Virginia University, 148 pp. [Available online at http:/etd.wvu.edu/ETDS/E2216/Xia_Jianjun_Dissertation.pdf.]